applied optics

Additive phase noise of fiber-optic links used in photonic microwave-generation systems

James P. Cahill,[1,*] Weimin Zhou,[1] and Curtis R. Menyuk[2]

[1]U.S. Army Research Laboratory, 2800 Powder Mill Rd, Adelphi, Maryland 20783, USA
[2]Department of Computer Science and Electrical Engineering, University of Maryland, Baltimore County, 1000 Hilltop Cir, Baltimore, Maryland 21250, USA
*Corresponding author: james.p.cahill15.civ@mail.mil

Received 27 July 2016; revised 21 September 2016; accepted 21 September 2016; posted 23 September 2016 (Doc. ID 272637); published 17 October 2016

In this work, we analyze the contributions of several mechanisms to the additive phase noise of the optical fiber in a microwave-photonic link. We discuss their fiber-length dependence and their impact on the phase noise of an optoelectronic oscillator. Furthermore, we present and verify for the first time a mechanism by which double-Rayleigh scattering directly generates microwave phase noise.

OCIS codes: (060.2360) Fiber optics links and subsystems; (060.5625) Radio frequency photonics; (120.5050) Phase measurement.

http://dx.doi.org/10.1364/AO.56.000B18

1. INTRODUCTION

The Army requires low phase noise signals to ensure high signal-to-noise ratios and narrow clutter blinds in its radar systems. This requirement is particularly challenging for radar systems with operating frequencies above a few gigahertz, because the phase noise of a signal increases when its frequency is multiplied. Quartz oscillators are the most common frequency reference; however, their output frequencies must be multiplied many times when they are used in high-frequency radar systems. Consequently, their phase noise is unacceptably high for many applications. The Army's requirements for frequency sources go beyond low phase noise. Frequency sources must also have low size, weight, power, and cost. All of these requirements must be taken into account when selecting the resonators with which to build the Army's next generation frequency sources.

Single-mode optical fibers are one candidate for frequency stabilization that meets these requirements. Their low loss per unit length allows signals to be delayed by tens to hundreds of microseconds. This capability has been exploited to stabilize the frequency of a continuous-wave laser to 7×10^{-15} at 1 s [1]. This performance approaches that of state-of-the-art optical cavities [2]. Moreover, single-mode optical fibers are readily and cheaply available as a commercial product, and kilometers-long spools can be miniaturized into volumes of less than 1 L.

One approach to generating a low-phase-noise microwave signal using a single-mode optical fiber is the optoelectronic oscillator (OEO) [3]. The OEO is a delay-line microwave oscillator, where the delay line is composed of a microwave–photonic (MW-photonic) link with a kilometers-long optical fiber. Hence, the phase noise of the OEO's output signal is easily related to the additive phase noise of the MW-photonic link that it is composed of. In the design of OEOs, it is sometimes possible to treat the optical fiber as an ideal microwave delay line. In this case, the phase noise is inversely proportional to the square of the optical fiber length [3]. This design paradigm is useful when the additive phase noise of the MW-photonic link is dominated by the additive noise of its electronic components, such as microwave amplifiers. However, as we will discuss in greater detail, the relationship between OEO phase noise and optical fiber length changes when additive noise from the optical fiber link contributes significantly to the MW-photonic link noise.

In this paper, we will summarize several previously reported sources of additive phase noise in the MW-photonic link and discuss their length dependence. We will analyze and experimentally verify for the first time a mechanism by which double-Rayleigh scattering (DRS) directly generates microwave phase noise with no intervening mechanisms. Finally, we will discuss the phase noise of an OEO and the impact of fiber-length dependent phase noise.

2. PREVIOUSLY REPORTED SOURCES OF ADDITIVE PHASE NOISE IN MICROWAVE–PHOTONIC LINKS

In this section, we will describe the additive phase noise that is induced in a MW-photonic link by sources within the optical fiber: thermodynamic fluctuations of the optical fiber, the conversion of optical intensity noise to microwave phase noise

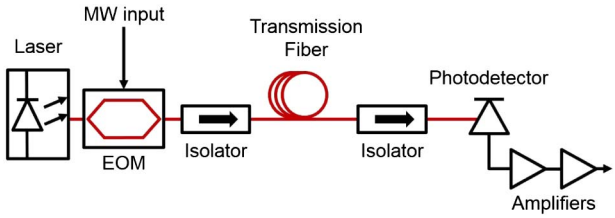

Fig. 1. Architecture of the MW-photonic link.

(including intensity noise induced by processes within the optical fiber), chromatic dispersion, and double scattering from discrete points. Environmental perturbations which affect the optical path length through the optical fiber, such as temperature fluctuations and vibrations, can also contribute to the additive phase noise of a MW-photonic link. However, a detailed analysis of their contribution is outside the scope of this paper.

There are several different architectures for a MW-photonic link. The most widespread architecture is the intensity-modulated direct detection (IMDD) link, so the analysis and results in this paper pertain to IMDD MW-photonic links. In Fig. 1, we show the architecture of an IMDD link.

The following conventions are used in this paper: the power spectral density of a quantity will be denoted by the symbol S. All power spectral densities are one-sided unless otherwise noted. We report the phase noise in the form of the single-sideband phase noise, which is defined as (1/2) the one-sided power spectral density of the phase noise, so that $\mathcal{L}(\omega) \equiv (1/2)S_\phi(\omega)$, where ω denotes the radial offset frequency.

A. Thermodynamic Fluctuations

The physical length and index of refraction of the optical fiber can change due to thermodynamic fluctuations, leading to variations in the group delay in the optical fiber. Hence, thermodynamic fluctuations impose a lower bound on the additive phase noise of an optical fiber [4–6].

The phase noise induced by thermodynamic fluctuations of the temperature, called the thermoconductive noise, is given by [6]

$$S_{\phi,\mathrm{TC}}(\omega) = \left(\frac{\omega_m}{c}\right)^2 \left(\frac{dn}{dT} + n\alpha_L\right)^2 L^2 S_{\delta T}(\omega), \tag{1}$$

where ω_m is the microwave frequency, n is the effective index of refraction of the optical fiber, dn/dT is the thermal coefficient of the index of refraction, α_L is the coefficient of thermal expansion, L is the length of the optical fiber, and $S_{\delta T}$ is the power spectral density of the temperature fluctuations:

$$S_{\delta T}(\omega) = \frac{k_B T^2}{4\pi^2 \kappa L} \mathrm{Re}\left[\exp\left(\frac{j\omega r_0^2}{2D}\right) E_1\left(\frac{j\omega r_0^2}{2D}\right)\right], \tag{2}$$

where k_B is Boltzmann's constant, T is the temperature, κ is the thermal conductivity, and D is the thermal diffusivity. We have $r_0^2 \equiv (1/2)w_0^2$, where w_0 is the mode-field radius of the fiber and E_1 is the exponential integral. Equation (1) shows an explicit L^2-dependence. However, because the power spectral density of the temperature fluctuations is inversely proportional to the optical fiber length, the thermoconductive noise is proportional to the first power of the optical fiber length.

B. Optical-AM-to-microwave-PM Conversion

Optical relative intensity noise (RIN)—including RIN occurring in the laser as well as RIN induced by processes within the optical fiber, such as DRS—can also contribute to the microwave phase noise via amplitude-to-phase noise (AM-PM) conversion in the photodetector or other microwave components [7–10]. The conversion coefficient is generally sensitive to several different parameters and should be measured empirically. We can determine the conversion coefficient from the derivative of the microwave phase with respect to the optical power, $d\phi/dP$. The optical intensity noise is typically reported as the RIN, which is measured in units relative to the average power. We find that the single-sideband phase noise due to AM-PM conversion, $\mathcal{L}_{\mathrm{AM\text{-}PM}}(\omega)$, is related to the power spectral density of the RIN by

$$\mathcal{L}_{\mathrm{AM\text{-}PM}}(\omega) = \frac{1}{2}\left(\frac{d\phi}{dP/P}\right)^2 S_{\mathrm{RIN}}(\omega). \tag{3}$$

Equation (3) shows no explicit dependence on the optical fiber length. The conversion of intensity noise to phase noise occurs in the optoelectronic and electronic components following the optical fiber, so the AM-PM conversion coefficient is not expected to depend on the fiber length. However, as noted in Section 2.D, the DRS-induced RIN at the output of an optical fiber will depend on the fiber-length [9,11,12].

C. Chromatic Dispersion

Chromatic dispersion causes the group velocity of light in an optical fiber to depend on the optical frequency. Hence, the laser's frequency noise will cause the group delay in the optical fiber to vary, generating microwave phase noise [13]. The microwave phase noise that is induced by this process is given by the expression

$$\mathcal{L}_{\mathrm{CD}}(\omega) = \frac{1}{2}\left(\frac{\omega_m \lambda^2 D_\lambda}{c}\right)^2 L^2 S_{\nu,\mathrm{laser}}(\omega), \tag{4}$$

where ω_m is the microwave frequency, λ is the laser wavelength, D_λ is the dispersion coefficient of the optical fiber, c is the speed of light, L is the length of the optical fiber, and $S_{\nu,\mathrm{laser}}(\omega)$ is the power spectral density of the laser frequency noise.

The dispersion-induced additive phase noise is proportional to the square of the optical-fiber length. For a typical single-mode optical fiber, SMF-28, the dispersion coefficient is $D_\lambda = 18$ ps/(nm · km). So, for a 10 GHz signal that is modulated onto light with a wavelength of 1550 nm, chromatic dispersion will lead to a phase noise contribution of $\mathcal{L}_{\mathrm{CD}}(\omega) = (1/2)(8 \times 10^{-29}\ \mathrm{s^2/m^2}) L^2 S_{\nu,\mathrm{laser}}(\omega)$.

D. Double Scattering from Discrete Points

Laser frequency noise is also converted to microwave phase noise via interference of the light that scatters twice from discrete points within a MW-photonic link, such as fiber connectors, splices, photodiode faces, or other interfaces. In contrast to the mechanisms previously discussed, double scattering does not directly lead to a variation of the group delay through an optical fiber. Instead the twice-scattered beam interferes with the unscattered light, so that the laser frequency noise generates microwave phase noise. The microwave phase noise that is

induced by this process is found by taking the Fourier transform of the autocorrelation function, which is given by [14]

$$r_{\phi,\mathrm{DS}}(\tau) = \eta^2 \sin[\omega_m \Delta\tau_z] W_\phi(\tau), \tag{5}$$

where η is the power ratio of the reflected and unreflected light, $\Delta\tau_z \equiv 2n(z_1 - z_2)/c$ is the round-trip time delay due to the reflections, n is the effective index of the optical fiber, and z_1 and z_2 denote the first and second reflection points, respectively. W_ϕ is given by

$$W_\phi(\tau) = \exp\left[-8\int_{-\infty}^{\infty} S_{\phi,L}(f)\sin^2(\pi f\tau)\sin^2(\pi f\Delta\tau_z)\mathrm{d}f\right], \tag{6}$$

where $S_{\phi,L}(f)$ is the two-sided power spectral density of the laser phase noise.

The phase noise due to double scattering from discrete points does not explicitly depend on the optical-fiber length. However, in many cases, the reflection points will be on opposite ends of the optical fiber. In this case, the additive phase noise has a complicated dependence on the optical-fiber length. A full discussion of the optical-fiber-length dependence of the phase noise is outside the scope of this paper; however, in some situations, the phase noise will increase as the optical-fiber length is increased [14]. Additionally, the microwave phase noise that is induced by this process is proportional to the reflectivity of the reflection points. Hence, it can be mitigated by inserting optical isolators immediately prior to reflection points or by using low-reflectivity connectors or splices.

3. ADDITIVE PHASE NOISE DUE TO DOUBLE RAYLEIGH SCATTERING

Even when the double scattering from discrete points is mitigated, double-scattering-induced microwave phase noise can arise from Rayleigh scattering—one of the fundamental phenomena that dominate the propagation loss of silica optical fibers. We refer to this phase noise as DRS-induced microwave phase noise. Because the scattering points in DRS are distributed throughout the optical fiber, the microwave phase noise that is generated by DRS cannot be mitigated using isolatorsor low-reflectivity components. In this section, we analyze a mechanism by which DRS directly leads to microwave phase noise.

Rayleigh scattering in optical fibers occurs due to spatial variations of the density of the optical fiber that are "frozen in" when the fiber is formed. A portion of the light traveling through an optical fiber will scatter from these density variations at an angle of approximately 180°, so that this portion of the light is guided by the optical fiber and propagates in the direction opposite to that of the incident light. A portion of the once-reflected light will undergo the same process a second time, so that there is a component of light that copropagates with the incident light but has been delayed by the path between the two scattering points. The interference between the double-scattered light and unscattered light modulates the intensity of the light, effectively becoming a source of optical RIN.

The power spectral density of the DRS-induced RIN [11,15,16] is found by taking the Fourier transform of the autocorrelation function, $r_{\mathrm{RIN}}(\tau)$,

$$r_{\mathrm{RIN}}(\tau) = 2T_p\sigma^4\int_0^L\int_0^{z_1} e^{-2\alpha\Delta z} W_\phi(\tau, z_1, z_2)\mathrm{d}z_2\mathrm{d}z_1, \tag{7}$$

where $T_p = (5/9)$ is a coefficient due to the randomly varying polarization [15,17], σ^2 is the Rayleigh reflection coefficient, α is the propagation loss factor of the optical fiber, and $\Delta z \equiv |z_2 - z_1|$ is the distance between the scattering points. The quantity $W_\phi(\tau, z_1, z_2)$ is defined by Eq. (6).

It was experimentally demonstrated that DRS-induced RIN couples into microwave phase noise in [18], but the physical mechanism for the coupling was not made clear. Here we analyze a mechanism that couples DRS-induced RIN into microwave phase noise. The analysis is similar to that used in [14]; however, in the case of DRS, we must integrate the contributions from scattering points that are distributed throughout the optical fiber.

We assume a MW-photonic link in which the microwave signal is modulated onto a laser with a Mach–Zehnder intensity modulator at quadrature bias and subsequently propagates through an optical fiber of length L. The electric field at the output of the laser is

$$A_\ell(t, z) = \tilde{A}_\ell e^{j(\omega_0 t - \beta z)} e^{j\phi(t)} e^{-\alpha z}, \tag{8}$$

where $\tilde{A}_\ell$ is the electric field magnitude, ω_0 is the optical frequency, β is the optical wavenumber, and $\phi(t)$ is the laser phase noise. After passing through the intensity modulator and propagating through the optical fiber, the electric field becomes [19]

$$A_0(t) = \tilde{A}[1 - je^{j\epsilon(t)}]e^{j(\omega_0 t - \beta L)} e^{j\phi(t)} e^{-\alpha L}, \tag{9}$$

where $\tilde{A} \equiv \tilde{A}_\ell/\sqrt{2}$, $\epsilon(t) \equiv (m/2)\sin[\omega_m t]$ is the microwave signal that is transmitted through the link, m is the modulation depth, and ω_m is the microwave frequency. We have assumed that the microwave signal is noiseless, because we are interested only in the additive phase noise of the MW-photonic link. We can use the Jacobi–Anger expansion to approximate the unscattered field as

$$A_0(t) \approx \tilde{A}[1 - j + m\sin(\omega_m t)]e^{j(\omega_0 t - \beta L)} e^{j\phi(t)} e^{-\alpha L}, \tag{10}$$

where we have assumed that the modulation depth is much less than 1, and we have neglected the contribution of harmonics of order 2 and higher. The intensity of the unscattered light is given by

$$I_0(t) = 2\tilde{A}^2 e^{-2\alpha L}[1 + m\sin(\omega_m t)]. \tag{11}$$

The electric field at the output of the optical fiber due to DRS is

$$A_{\mathrm{DRS}}(t) = \tilde{A}\int_0^L\int_0^{z_1} \kappa(z_1)\kappa(z_2)A_0(t - \Delta\tau_z) \times e^{-\alpha(L + 2\Delta z)}\mathrm{d}z_2\mathrm{d}z_1, \tag{12}$$

where $\kappa(z)$ is a zero-mean random variable describing the variation of the index of refraction, as described in [20]. It is defined by the following relations:

$$\langle\kappa(x)\kappa^*(y)\rangle = \begin{cases} 0, & \text{if } x \neq y \\ \sigma^2, & \text{if } x = y \end{cases},$$
$$\langle\kappa(x)\kappa(y)\rangle = 0, \qquad \text{for all } x, y, \tag{13}$$

where σ^2 is the Rayleigh reflectivity coefficient.

The contribution of higher-order scattering effects to the electric field is neglected. Hence, the total electric field at the output of the optical fiber is found by adding Eqs. (9) and (12).

The total intensity of the light at the output of the optical fiber is

$$I_{\mathrm{tot}}(t) = |A_0(t)|^2 + |A_{\mathrm{DRS}}(t)|^2 + A_{\mathrm{DRS}}(t)A_0^*(t) + A_{\mathrm{DRS}}^*(t)A_0(t). \tag{14}$$

The first term in Eq. (14) is the intensity of the unscattered light, which is given by Eq. (11). The second term is due to noise–noise beating, and its magnitude is sufficiently small that we can neglect it. The third and fourth terms are complex conjugates of each other, and they take the form

$$\begin{aligned} A_{\mathrm{DRS}}(t)A_0^*(t) = \tilde{A}^2 e^{-2\alpha L} \iint \kappa(z_1)\kappa(z_2) \\ \times [2 + (1+j)\sin(\omega_m t) \\ + (1-j)\sin(\omega_m t - \omega_m \Delta\tau_z)]e^{-j\Phi(t)} \\ \times e^{-2\alpha\Delta z}\mathrm{d}z_2\mathrm{d}z_1, \end{aligned} \tag{15}$$

where we let $\Phi \equiv \phi(t) - \phi(t-\Delta\tau_z) + \omega_m\Delta\tau_z$.

In order to find the microwave phase noise, we first neglect all of the time-invariant contributions to the intensity. Then, by combining Eqs. (11), (14), and (15), we find

$$\begin{aligned} \frac{I_{\mathrm{tot}}(t)}{m\tilde{A}^2 e^{-2\alpha L}} = 2\sin(\omega_m t) \\ + \iint e^{-2\alpha\Delta z}\kappa(z_1)\kappa(z_2)[(1+j)\sin(\omega_m t) \\ + (1-j)\sin(\omega_m t - \omega_m\Delta\tau_z)]e^{-j\Phi(t)}\mathrm{d}z_2\mathrm{d}z_1 \\ + \iint e^{-2\alpha\Delta z}\kappa^*(z_1)\kappa^*(z_2)[(1-j)\sin(\omega_m t) \\ + (1+j)\sin(\omega_m t - \omega_m\Delta\tau_z)]e^{j\Phi(t)}\mathrm{d}z_2\mathrm{d}z_1, \end{aligned} \tag{16}$$

where all of the remaining terms oscillate at the microwave frequency, ω_m. The sum of an arbitrary number, N, of sinusoids that oscillate at the same frequency, ω_m, can be represented by a single effective sinusoid according to the following identity:

$$a_{\mathrm{tot}}\sin(\omega_m t + \theta_{\mathrm{tot}}) = \sum_i a_i \sin(\omega_m t + \theta_i), \tag{17}$$

where i takes integer values from 1 to N. The additive phase noise of the MW-photonic link is then found by the equation

$$\theta_{\mathrm{tot}} \equiv \tan^{-1}\left[\frac{\sum_i a_i \sin(\theta_i)}{\sum_i a_i \cos(\theta_i)}\right]. \tag{18}$$

We note that the first term in Eq. (16) will only contribute to the denominator of Eq. (18). Moreover, the magnitude of all other terms is much less than one. Hence, the additive phase noise of the MW-photonic link is approximately

$$\theta_{\mathrm{tot}} \approx \frac{1}{2}\sum_i a_i \sin(\theta_i). \tag{19}$$

Combining Eqs. (16), (17), and (19), we find that the additive phase noise of the MW-photonic link is

$$\theta_{\mathrm{tot}}(t) = \frac{1-j}{2}\iint \kappa(z_1)\kappa(z_2)\sin(\omega_m\Delta\tau_z)e^{-j\Phi(t)}e^{-2\alpha\Delta z}\mathrm{d}z_2\mathrm{d}z_1 + \mathrm{c.c.} \tag{20}$$

The power spectral density of the additive phase noise can be found by taking the Fourier transform of the autocorrelation of the phase, $r_\theta(\tau) \equiv \langle\theta_{\mathrm{tot}}(t)\theta_{\mathrm{tot}}^*(t+\tau)\rangle$. The autocorrelation can be shown to be

$$r_\theta(\tau) = T_P\sigma^4 \iint \sin^2(\omega_m\Delta\tau_z)e^{-2\alpha\Delta z}W_\phi(\tau, z_1, z_2)\mathrm{d}z_2\mathrm{d}z_1, \tag{21}$$

where W_ϕ is defined by Eq. (6), and we have added the coefficient T_P to account for the degree of polarization of the scattered light, as in the case of the DRS-induced RIN [11,15,17].

For realistic signals, the factor $\sin^2(\omega_m\Delta\tau_z)$ varies more rapidly with respect to z_1 and z_2 than does W_ϕ. We approximate the rapidly varying term by its average value, so that $\sin^2(\omega_m\Delta\tau_z) \approx (1/2)$. The autocorrelation becomes

$$r_\theta(\tau) = \frac{T_P\sigma^4}{2}\iint e^{-2\alpha\Delta z}W_\phi(\tau, z_1, z_2)\mathrm{d}z_2\mathrm{d}z_1. \tag{22}$$

By comparing Eqs. (7) and (22), we find that the autocorrelation function of the DRS-induced microwave phase noise differs from the autocorrelation of the DRS-induced RIN by a factor of (1/4). When we compare the power spectral density of the DRS-induced RIN, S_{RIN}, to the single-sideband phase noise, $\mathcal{L}_{\mathrm{DRS}}$, there is an additional factor of (1/2), because of the definition of the single-sideband phase noise. Hence, the length dependence of the DRS-induced phase noise will be the same as the length dependence of the DRS-induced RIN. A full discussion of the length dependence of the DRS-induced noise is outside the scope of this paper. Nonetheless, it has been shown that for optical-fiber lengths below some value, the DRS-induced phase noise can grow superlinearly over certain ranges of offset frequency. For optical-fiber lengths above that value, the phase noise grows linearly or sublinearly with respect to the fiber length. The transition between these two regions is determined by the magnitude of the laser phase noise [11,12,16]. Finally, we note that the similarity between the DRS-induced RIN and phase noise is not a coincidence; the contributions to both noise types arise from the same physical process.

4. EXAMPLE MW-PHOTONIC LINK

In this section, we will examine the contributions of each of the above noise sources to an example MW-photonic link. As noted before, we are not studying here the phase noise that is due to ambient environmental perturbations. However, we note that these fluctuations often dominate the phase noise of the link at offset frequencies below 100 Hz.

We show the link architecture in Fig. 1. A distributed feedback (DFB) laser emits light at 1550 nm with an output power of 80 mW. A 10-GHz bandwidth, X-cut $LiNbO_3$ electro-optic modulator (EOM) modulates the intensity of the laser with the input microwave signal. The modulated light is transmitted through a 6-km long spool of single-mode optical fiber. After

exiting the optical fiber, the modulated light illuminates a 10-GHz-bandwdith $p-i-n$ photodetector. The resulting photocurrent passes through two low-phase noise 10-GHz amplifiers. On either side of the optical fiber are optical isolators. The isolator that is placed between the EOM and the entrance of the optical fiber reduces the magnitude of the backward-scattered light that enters the laser, thereby mitigating feedback effects. The isolator that is placed at the exit of the optical fiber reduces the magnitude of reflections from the photodetector interface that re-enter the optical fiber, thereby mitigating the contribution to the microwave phase noise of reflections from this point.

A. Link Parameters

In order to carry out the calculations that we described in the previous section, we must define several parameters that characterize the optical fiber. Table 1 summarizes these parameters.

In addition to these parameters, we must also measure the laser phase noise, the optical intensity noise, and the AM-PM conversion coefficient of the photodetector and microwave amplifiers.

We measured the laser phase noise using an asymmetric Mach–Zehnder interferometer with a path length difference of 3 cm, following the method of [13]. Figure 2 compares the measured laser phase noise to a numerical fit of the form $S_{\phi,L}(\omega) = S_0/\omega^2 + k/\omega^3$, where S_0 is $8.69 \times 10^5 (\text{rad/s})^2/\text{Hz}$ and k is $2.37 \times 10^{11} (\text{rad/s})^3/\text{Hz}$. The numerical fit diverges from the experimental data for offset frequencies lower than approximately 1 kHz. This trend indicates that there is a steeper component to the laser phase noise, which becomes visible at these offset frequencies.

Table 1. Single-mode Optical Fiber Parameters

Name	Symbol	Value
Thermal coefficient	$\frac{dn}{dT}$	9.488×10^{-6} K^{-1}
Linear expansion coef.	α_L	5×10^{-7} K^{-1}
Propagation loss	α	0.19 dB/km
Effective index	n_{eff}	1.47
Boltzmann constant	k_B	1.38×10^{-23} J/K
Thermal conductivity	κ	1.37 W/(m · K)
Thermal diffusivity	D	8.2×10^{-7} m^2/s
Dispersion coefficient	D_λ	18 ps/(nm · km)
Mode-field radius	w_0	5.2 μm
Rayleigh coefficient	σ^2	6.1×10^{-8} m^{-1}

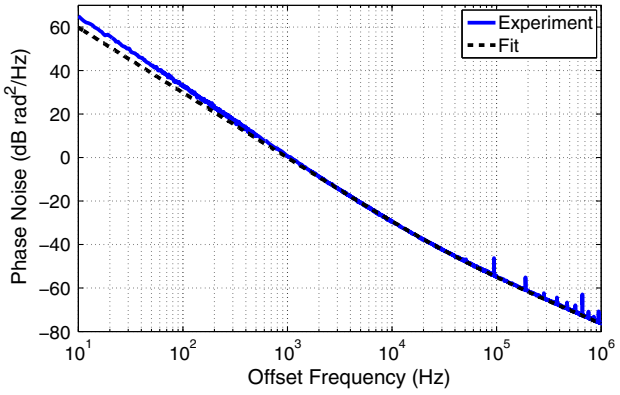

Fig. 2. Comparison of experimental measurement of and numerical fit to the laser phase noise.

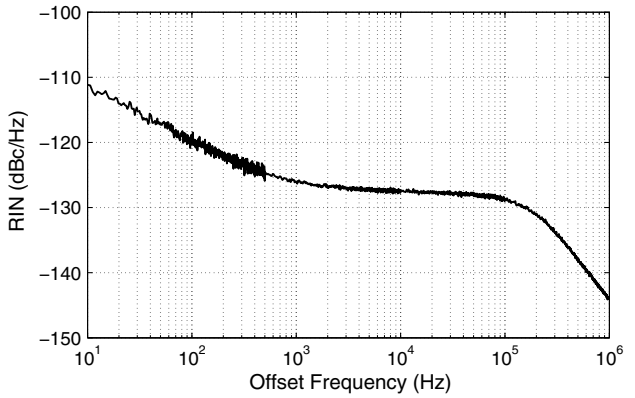

Fig. 3. Experimental measurement of the relative intensity noise induced by DRS in a 6-km single-mode optical fiber.

We measured the optical intensity noise in a similar fashion to [21]. A DFB laser emits light that propagates through 6 km of single-mode optical fiber. The light exiting the optical fiber illuminates a photodiode, and the photocurrent that is excited passes through a custom-built low-noise AC-coupled baseband amplifier that has a frequency range of 10 Hz to 10 MHz. We measured the power spectral density using a vector signal analyzer. Since the DRS-induced intensity noise is orders of magnitude higher than the laser RIN, we did not require the use of cross-correlation. We show our results in Fig. 3.

We directly measured the optical-intensity to microwave-phase conversion of the photodetector and microwave amplifier chain using a vector network analyzer to record the phase of a 10-GHz signal passing through the MW-photonic link. The measurement architecture is shown in Fig. 4. The output of the laser passes through an EOM. A network analyzer generates a 10-GHz signal, which passes through two amplifiers and a bandpass filter (BPF) with a center frequency of 10 GHz. The amplifiers and BPF are the same components that were used in the MW-photonic link (see Fig. 1). The 10 GHz signal then modulates the light that passes through the EOM. The modulated light passes through a variable optical attenuator and illuminates a photodetector. The photocurrent enters the network analyzer, which measures the phase difference between the input and output signals. In order to find the coefficient of optical-intensity to microwave-phase conversion, we fit a third-order polynomial to the microwave phase and calculated its derivative with respect to the optical power. The resulting curve

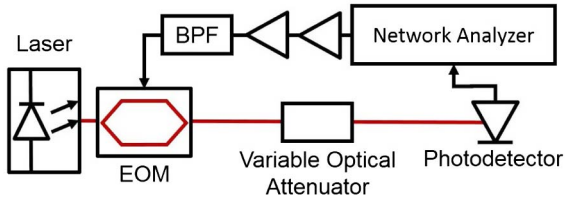

Fig. 4. Architecture of the AM-PM conversion measurement system.

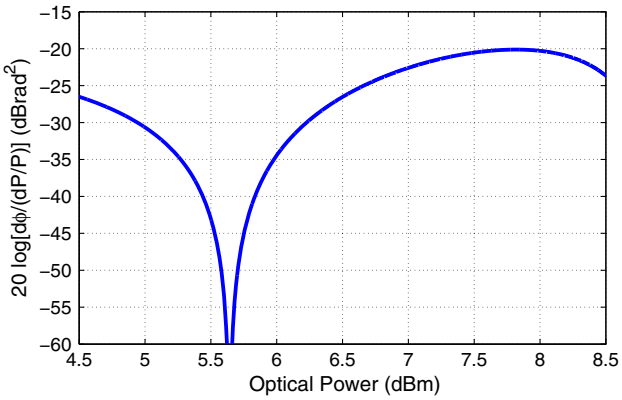

Fig. 5. Experimental results for the optical relative-intensity-noise to microwave-phase-noise conversion coefficient.

is then multiplied by the input optical power to obtain the quantity $d\phi/(dP/P)$. The results are plotted in Fig. 5. The MW-photonic link in this section was operated with optical power of approximately 6.75 dBm into the photodetector. This power level corresponds to an AM-PM coefficient of −24.3 dB.

B. Calculated Phase Noise

Figure 6 shows the expected contributions to the additive phase noise of the MW-photonic link from DRS (blue), AM-PM conversion (green), dispersion (red), and thermoconductive noise (light blue).

The results show that for this particular MW-photonic link, we expect the DRS-induced phase noise to dominate the additive phase noise. This result is highly dependent on the parameters of the MW-photonic link and will not be generally true. In particular, different lasers have vastly different phase noise and RIN. Moreover, the AM-PM conversion factor of the link can vary by orders of magnitude based on the value of the optical power or the bias voltage of the photodetector [8]. Each of these parameters has a strong influence on which fiber mechanisms dominate the additive phase noise of the MW-photonic link.

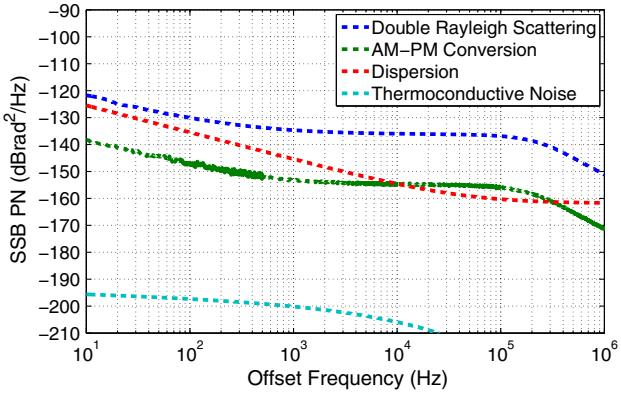

Fig. 6. Calculated results for the additive microwave phase noise due to DRS, AM-to-PM conversion, dispersion, and thermoconductive noise.

C. Experimental Results

In order to confirm the results of the previous section, we measured the additive phase noise of the link. As shown in Fig. 7, we used an additive phase noise measurement system, in which a low-phase-noise input signal is split two ways, so that one portion propagates through the device under test and its phase is compared to the phase of the other portion of the signal. This architecture is advantageous, because it rejects the phase noise of the input signal.

In our experiment, the device under test is a MW-photonic link, shown in Fig. 1, that delays the signal that passes through it by approximately 30 μs. If the two arms of the additive phase noise measurement system had a relative delay of that magnitude, the rejection of the input signal's phase noise would be drastically reduced. So, we inserted an identical MW-photonic link in the second arm of the phase noise measurement system in order to balance the relative delay between the two arms. To ensure that the phase noise that we measured was dominated by only one of the two MW-photonic links, we modulated the frequency of the laser in one of the MW-photonic links. This modulation mitigated the DRS-induced phase noise in one link, so that the phase noise of the other link was significantly higher. It is the phase noise of the unmodulated link that dominated the measured phase noise.

Figure 8 compares the experimental results (solid black line) to the calculated results (dashed blue line). For the range of offset frequencies from approximately 500 Hz to 1 MHz, the calculated results agree with the experimental results to within a factor of 2 dB. Hence, for these offset frequencies, the additive phase noise of this MW-photonic link is

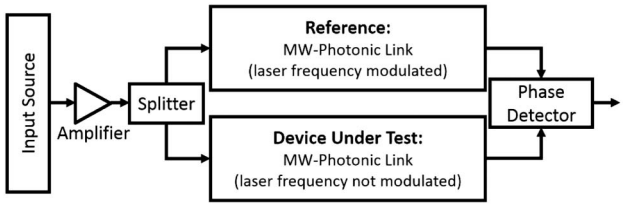

Fig. 7. Architecture of the additive phase noise measurement system.

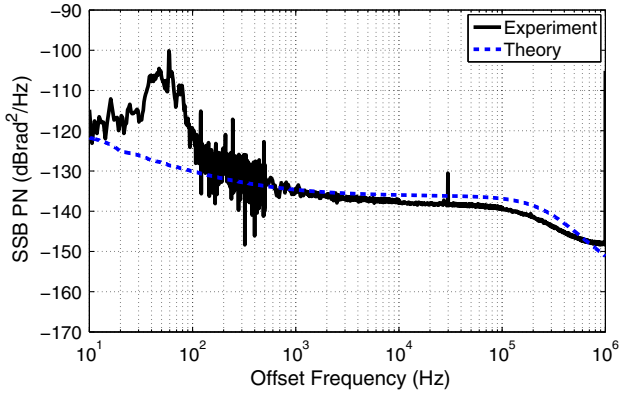

Fig. 8. Comparison of calculated and experimental results for the additive phase noise of the MW-photonic link.

dominated by the DRS-induced phase noise. For the range of offset frequencies from 10 Hz to approximately 500 Hz, the additive phase noise is dominated by the phase noise contributions of environmental fluctuations, which we did not take into consideration.

5. FIBER-BASED OPTO-ELECTRONIC OSCILLATORS

The OEO uses the stability of an optical fiber in order to generate a microwave signal [3]. As shown in Fig. 9, the basic architecture of an optical-fiber-based OEO is the same as that of a MW-photonic link, where the output of the photodetector has been connected with the input of the EOM so as to form a feedback loop. When the net small-signal gain of the OEO loop is greater than one, noise generated in the loop will create a self-sustaining microwave oscillation.

The critical parameter that characterizes the performance of an oscillator is its phase noise. The phase noise of an OEO, $\mathcal{L}_{\mathrm{OEO}}$, has a simple relationship with the additive phase noise of the MW-photonic link, $\mathcal{L}_{\mathrm{Link}}$ [3,22]. This relationship is given by

$$\mathcal{L}_{\mathrm{OEO}}(\omega) = \frac{\mathcal{L}_{\mathrm{Link}}(\omega)}{4\sin^2\left[\frac{\omega\tau_d}{2}\right] + \left(\frac{4\omega}{\Delta\omega_f}\right)\sin[\omega\tau_d] + \left(\frac{2\omega}{\Delta\omega_f}\right)^2}, \quad (23)$$

where $\tau_d \approx nL/c$ is the group delay through the OEO and $\Delta\omega_f$ is the bandwidth of the microwave BPF.

Hence, the results of the previous sections regarding MW-photonic links are directly applicable to analyzing the phase noise of an OEO. For example, Fig. 10 shows the expected phase noise of an OEO based on the 6-km-long MW-photonic link characterized in Section 4. The figure was generated by applying the transfer function of Eq. (23) to the experimentally measured additive phase noise shown in Fig. 8. We used a BPF bandwidth of 10 MHz.

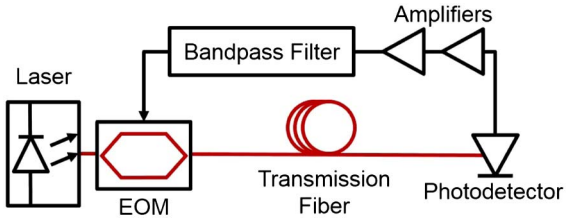

Fig. 9. Experimental setup of an OEO based on a MW-photonic link.

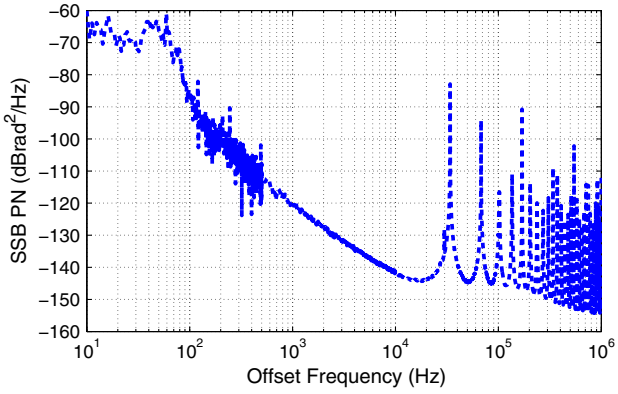

Fig. 10. Expected phase noise of an OEO built with the MW-photonic link characterized in Section 4.

When the offset frequency satisfies $\omega\tau_d \ll 1$, Eq. (23) reduces to

$$\mathcal{L}_{\mathrm{OEO}}(\omega) \approx \left(\frac{c}{n\omega L}\right)^2 \mathcal{L}_{\mathrm{Link}}(\omega). \quad (24)$$

Hence, the length-dependence of the OEO phase noise will be equivalent to that of the MW-photonic link reduced by a power of two. Notably, when the phase noise of the MW-photonic link is constant with the optical-fiber length, we find $\mathcal{L}_{\mathrm{OEO}}(\omega) \propto L^{-2}$. Indeed, this is the case when the additive phase noise of the MW-photonic link is dominated by the microwave components, and, in this case, increasing the optical-fiber length will reduce the microwave phase noise.

However, when the noise induced by the optical fiber contributes significantly to the additive phase noise of the link, the OEO phase noise may no longer scale as L^{-2}. In particular, when the noise of the microwave link grows in proportion to the second (or higher) power of the optical fiber, increasing the length of the fiber in the OEO will not reduce its phase noise. For example, in the case of chromatic dispersion we found that the phase noise of the MW-photonic link scales according to $\mathcal{L}_{\mathrm{CD}}(\omega) \propto L^2$. So, if the phase noise of a MW-photonic link is dominated by chromatic dispersion, the phase noise of an OEO that is constructed with that link will be independent of the optical fiber length.

In the case of DRS, we found that when the optical fiber length is above some value, the noise grows in direct proportion or sublinearly with respect to the fiber length, whereas when the optical fiber length is below some value, the noise can grow superlinearly. Hence, for a DRS-noise-dominated OEO, increasing the fiber length will reduce the OEO phase noise more efficiently when the length is above the critical value. This value depends on the laser phase noise. For a laser with a linewidth <5 kHz, the critical length was approximately 10 km [11,12,16].

Thus, simply increasing the optical fiber length in a MW-photonic link that forms an OEO may not be a sufficient measure to reduce the OEO's phase noise. Instead, one must identify and mitigate the dominant noise sources of the MW-photonic link as outlined in this paper.

6. FUTURE CONSIDERATIONS AND CONCLUSIONS

Because of its commercial availability and proven frequency stabilization capabilities, single-mode optical fiber is a promising candidate for use as a frequency stability reference for the Army. In this paper, we described several phase noise sources within the optical fiber of a MW-photonic link that generate optical-fiber-length-dependent phase noise. We analyzed and experimentally verified a mechanism by which DRS contributes directly to the additive phase noise of a MW-photonic link.

The OEO leverages the stability of an optical fiber to generate a low-phase-noise microwave signal. When noise sources

that are independent of the optical fiber length are the dominant contributors to the OEO phase noise, the OEO phase noise is inversely proportional to the square of the optical fiber length. However, when length-dependent noise sources contribute significantly to the noise of an OEO, increasing the optical fiber length may no longer reduce the OEO phase noise. In this case, the dominant noise sources must be identified and mitigated by other means.

REFERENCES

1. J. Dong, Y. Hu, J. Huang, M. Ye, Q. Qu, T. Li, and L. Liu, "Subhertz linewidth laser by locking to a fiber delay line," Appl. Opt. **54**, 1152–1156 (2015).
2. S. Häfner, S. Falke, C. Grebing, S. Vogt, T. Legero, M. Merimaa, C. Lisdat, and U. Sterr, "8×10^{-17} fractional laser frequency instability with a long room-temperature cavity," Opt. Lett. **40**, 2112–2115 (2015).
3. X. S. Yao and L. Maleki, "Optoelectronic microwave oscillator," J. Opt. Soc. Am. B **13**, 1725–1735 (1996).
4. K. H. Wanser, "Fundamental phase noise limit in optical fibers due to temperature fluctuations," Electron. Lett. **28**, 53–54 (1992).
5. S. Foster, A. Tikhomirov, and M. Milnes, "Fundamental thermal noise in distributed feedback fiber lasers," IEEE J. Quantum Electron. **43**, 378–384 (2007).
6. L. Duan, "General treatment of the thermal noises in optical fibers," Phys. Rev. A **86**, 023817 (2012).
7. K. J. Williams, R. D. Esman, and M. Dagenais, "Effects of high space-charge fields on the response of microwave photodetectors," IEEE Photon. Technol. Lett. **6**, 639–641 (1994).
8. J. Taylor, S. Datta, A. Hati, C. Nelson, F. Quinlan, A. Joshi, and S. Diddams, "Characterization of power-to-phase conversion in high-speed P-I-N photodiodes," IEEE Photon. J. **3**, 140–151 (2011).
9. A. Docherty, C. R. Menyuk, J. P. Cahill, O. Okusaga, and W. Zhou, "Rayleigh-scattering-induced RIN and amplitude-to-phase conversion as a source of length-dependent phase noise in OEOs," IEEE Photon. J. **5**, 5500514 (2013).
10. O. Okusaga, J. P. Cahill, A. Docherty, C. R. Menyuk, W. Zhou, and G. M. Carter, "Suppression of Rayleigh-scattering-induced noise in OEOs," Opt. Express **21**, 22255–22262 (2013).
11. M. Fleyer, S. Heerschap, G. A. Cranch, and M. Horowitz, "Noise induced in optical fibers by double Rayleigh scattering of a laser with $1/f^{\nu}$ frequency noise," Opt. Lett. **41**, 1265–1268 (2016).
12. J. P. Cahill, O. Okusaga, W. Zhou, C. R. Menyuk, and G. M. Carter, "Superlinear growth of Rayleigh scattering-induced intensity noise in single-mode fibers," Opt. Express **23**, 6400–6407 (2015).
13. K. Volyanskiy, Y. K. Chembo, L. Larger, and E. Rubiola, "Contribution of laser frequency and power fluctuations to the microwave phase noise of optoelectronic oscillators," J. Lightwave Technol. **28**, 2730–2735 (2010).
14. W. Shieh and L. Maleki, "Phase noise of optical interference in photonic RF systems," IEEE Photon. Technol. Lett. **10**, 1617–1619 (1998).
15. P. Wan and J. Conradi, "Impact of double Rayleigh backscatter noise on digital and analog fiber systems," J. Lightwave Technol. **14**, 288–297 (1996).
16. M. Fleyer, J. P. Cahill, M. Horowitz, C. R. Menyuk, and O. Okusaga, "A comprehensive model for studying noise induced by self-homodyne detection of backward Rayleigh scattering," Opt. Express **23**, 25635–25652 (2015).
17. M. O. van Deventer, "Polarization properties of Rayleigh backscattering in single-mode fibers," J. Lightwave Technol. **11**, 1895–1899 (1993).
18. J. P. Cahill, O. Okusaga, W. Zhou, C. R. Menyuk, and G. M. Carter, "Effect of optical scattering on one-way RF frequency transfer over optical fibers," in *Proceedings of Precise Time and Time Interval Systems and Applications Meeting* (2013).
19. A. Yariv and P. Yeh, *Photonics: Optical Electronics in Modern Communications*, 6th ed. (Oxford University, 2007), p. 426, for more details on the electric field that emerges from a Mach–Zehnder interferometer.
20. P. Gysel and R. K. Staubli, "Statistical properties of Rayleigh backscattering in single-mode fibers," J. Lightwave Technol. **8**, 561–567 (1990).
21. E. Rubiola, K. Volyanskiy, and L. Larger, "Measurement of the laser relative intensity noise," in *Proceedings of International Frequency Control Symposium Joint with the 22nd European Frequency and Time Forum* (2009).
22. Y. K. Chembo, K. Volyanskiy, L. Larger, E. Rubiola, and P. Colet, "Determination of phase noise spectra in optoelectronic microwave oscillators: a Langevin approach," IEEE J. Quantum Electron. **45**, 178–186 (2009).